

**Protection of DNA by metal ions at 95°C: from lower critical solution temperature (LCST) behavior to coordination-driven self-assembly**

Chang Lu<sup>1,2</sup>, Yuancong Xu<sup>2,3</sup>, Po-Jung Jimmy Huang<sup>2</sup>, Mohamad Zandieh<sup>2</sup>, Yihao Wang<sup>2</sup>, Jinkai Zheng<sup>1</sup> and Juewen Liu<sup>2,\*</sup>

1. Institute of Food Science and Technology, Chinese Academy of Agricultural Sciences, Beijing 100193, P. R. China

2. Department of Chemistry, Waterloo Institute for Nanotechnology, University of Waterloo, Waterloo, Ontario, Canada

Email: liujw@uwaterloo.ca

3. Beijing Advanced Innovation Center for Food Nutrition and Human Health, College of Food Science & Nutritional Engineering, China Agricultural University, Beijing, China

## Abstract

While polyvalent metal ions and heating can both degrade nucleic acids, we herein report that a combination of them leads to stabilization. After incubating 4 mM various metal ions and DNA oligonucleotides at 95°C for 3 h at pH 6 or 8, metal ions were divided in four groups based on gel electrophoresis results.  $\text{Mg}^{2+}$  can stabilize the DNA at pH 6 without forming stable nanoparticles at room temperature.  $\text{Co}^{2+}$ ,  $\text{Cu}^{2+}$ ,  $\text{Cd}^{2+}$ ,  $\text{Mn}^{2+}$  and  $\text{Zn}^{2+}$  all protected the DNA and formed nanoparticles, whereas the nanoparticles formed with  $\text{Fe}^{2+}$  and  $\text{Ni}^{2+}$  were so stable that they remained even in the presence of EDTA. At pH 8,  $\text{Ce}^{3+}$  and  $\text{Pb}^{2+}$  showed degraded DNA bands. For  $\text{Mg}^{2+}$ , better protection was achieved with higher metal and DNA concentrations. By monitoring temperature-programmed fluorescence change, a sudden drop in fluorescence intensity attributable to the lower critical solution temperature (LCST) transition of DNA was found to be around 80°C for  $\text{Mg}^{2+}$ , while this transition temperature decreased with increasing  $\text{Mn}^{2+}$  concentration. The unexpected thermal stability of DNA enabled by metal ions is useful for extending the application of DNA at high temperatures, forming coordination-drive nanomaterials, and it might offer insights into the origin of life of the early earth.

## Introduction

The application of nucleic acids have drastically expanded over the last few decades to various fields such as biosensors, nanotechnology and materials science.<sup>1-6</sup> DNA has very high stability, RNA is less stable, while both have programmable structures, catalytic activities and molecular recognition functions.<sup>7,8</sup> For practical applications and fundamental insights, preserving and understanding the stability of nucleic acids is critical.

Nucleic acids can be cleaved by acids, bases, heating and nucleases.<sup>9,10</sup> While DNA is in general quite resistant to high temperature, as demonstrated in polymerase chain reactions (PCR), prolonged heating can still cleave DNA.<sup>11</sup> Heat-induced DNA damages include DNA strand breaks, hydrolysis of glycosyl bonds with depurination, and deamination of cytosine.<sup>12</sup> Metal ions and metal complexes are often used to cleave DNA.<sup>13</sup> Many metal ions such as  $\text{Ce}^{4+}$ ,  $\text{Co}^{2+}$ ,  $\text{Co}^{3+}$ ,  $\text{Fe}^{3+}$ ,  $\text{Ni}^{2+}$ ,  $\text{Mo}^{4+}$ ,  $\text{Pd}^{2+}$ ,  $\text{Zr}^{4+}$  and trivalent lanthanides are considered as hydrolytic agents.<sup>14,15</sup> Metal-induced RNA cleavage has been used as a structural probing method.<sup>16</sup> Some single-strand nucleic acids can bind certain metal ions and exhibit catalytic activities for DNA or RNA cleavage.<sup>17-19</sup>

While heating and metal ions can individually cleave nucleic acids, interestingly, recent work from the Li group showed that  $\text{Fe}^{2+}$  ions can coordinate with DNA oligonucleotides to form nanoparticles by heating at  $95^\circ\text{C}$  for 3 h.<sup>20-24</sup> In addition,  $\text{Zn}^{2+}$  can form similar nanoparticles after prolonged heating with various types of RNA,<sup>25</sup> where the RNA/ $\text{Zn}^{2+}$  nanoparticles retained the integrity of RNA. These intriguing results led us to explore the stability of DNA with the combined effect of heating and metal ions. Metal coordination by biomolecules has been an attractive method to produce functional nanomaterials.<sup>21,26-29</sup> In addition, the thermal stability of DNA is critical for some hypothesis in the origin of life,<sup>30,31</sup> and building DNA-based data storage systems.<sup>32</sup> Using gel electrophoresis to characterize the stability of DNA and fluorescence spectroscopy to follow the assembly of DNA, we herein report a few different types of metal ions, most of which could protect DNA at close to boiling temperature.

## Materials and Methods

**Chemicals.** All the DNA samples were purchased from Integrated DNA Technologies (Coralville, IA, USA). The sequence of the FAM-labeled 24-mer DNA is 5'-FAM-ACG CAT CTG TGA AGA GAA CCT GGG. All the metals (chloride salts) and buffer were purchased from

Sigma-Aldrich and Mandel Scientific (Guelph, Ontario, Canada), respectively. Milli-Q water was used to prepare all buffers and solutions.

**Heating of DNA.** The heating experiment was performed in a PCR thermocycler for up to 3 h. In a typical experiment, the DNA samples was prepared by mixing 3  $\mu\text{M}$  24-mer DNA (non-labeled) and 1  $\mu\text{M}$  carboxyfluorescein (FAM)-labeled DNA of the same sequence. 40  $\mu\text{L}$  of the DNA sample was mixed with 10  $\mu\text{L}$  ion (20 mM) solution. The samples were then heated at 95°C for 3 h.

**Gel electrophoresis.** After heating, 2  $\mu\text{L}$  products was mixed with 18  $\mu\text{L}$  gel loading buffer (0.1 $\times$ loading dye, 5 mM EDTA, 8 M urea), and the samples were then separated by 15% denaturing polyacrylamide gel electrophoresis (dPAGE) at 200 V for 80 min. The gels were analyzed using a Bio-Rad ChemiDoc MP imaging system.

**DNA release.** The stability of the coordination nanoparticles was evaluated by fluorescence recovery. 100  $\mu\text{L}$  sample (DNA and  $\text{Mn}^{2+}/\text{Fe}^{2+}$  after heating) was added in a 96 well microplate. Then the kinetics of DNA release was studied by adding 2  $\mu\text{L}$  of 1 M KCN, 1 M KSCN, 250 mM EDTA or 250 mM sodium tripolyphosphate (STPP) at 25°C. The fluorescence was measured using a Tecan Spark microplate reader with 485 nm excitation and 530 nm emission. The fluorescence of the samples was recorded using a digital camera with excitation at 470 nm in a dark room.

**Real-time fluorescence monitoring during heating.** The transition temperature of the DNA-metal ion mixture was measured in Bio-Rad CFX-96 real-time PCR thermocycler. The samples were initially equilibrated at 20°C for 10 min before gradually raising the temperature to 95°C with 1°C interval every 10 sec. For each 20  $\mu\text{L}$  sample, 0.4  $\mu\text{M}$  FAM-24mer was used for monitoring the fluorescence in 5 mM MOPS, pH 8.0. In the DNA concentration-dependent study, each sample contained 4 mM metal ions with additional non-labeled DNA added. On the other hand, total of 4  $\mu\text{M}$  DNA was used for each sample for the metal concentration-dependent study.

## Results and Discussion

**Thermal degradation of DNA is faster at lower pH.** Before examining the effect of metal ions, we first tested the effect of pH. DNA is known to be less stable at lower pH due to depurination-induced cleavage.<sup>33</sup> The pH of water is lowered at higher temperature,<sup>34</sup> which may further

contribute to heating-induced DNA cleavage. We first tested the thermal stability of a metal-free FAM-labeled 24-mer random sequenced DNA (1  $\mu\text{M}$ ) at different pH. After incubation the DNA at 95°C for 3 h, the samples were analyzed by denaturing polyacrylamide gel electrophoresis (dPAGE, Figure 1A). The DNA degraded at pH 6 or lower with full degradation observed at pH 3 and 4, but it was stable at pH 7 and 8. Therefore, when studying the effect of metal ions, the effect of pH needs to be considered and controlled.

**Metal protection of DNA at 95°C (pH 6.0).** We then studied the thermal stability of the DNA in the presence of ten common polyvalent metal ions including  $\text{Mg}^{2+}$ ,  $\text{Co}^{2+}$ ,  $\text{Cu}^{2+}$ ,  $\text{Zn}^{2+}$ ,  $\text{Mn}^{2+}$ ,  $\text{Ni}^{2+}$ ,  $\text{Cd}^{2+}$ ,  $\text{Pb}^{2+}$ ,  $\text{Fe}^{2+}$  and  $\text{Ce}^{3+}$  (4 mM each). We chose 4 mM since it was used for making the Fe/DNA coordination nanoparticles.<sup>20</sup> The DNA was a mixture of 1  $\mu\text{M}$  FAM-24mer DNA and 3  $\mu\text{M}$  non-labeled DNA of the same sequence. After incubation the samples at 95°C for 3 h in 5 mM pH 6 MES buffer, most of the transition metal containing samples precipitated. We chose 5 mM buffer concentration since it showed a very high protection effect by  $\text{Mg}^{2+}$  and the optimization of buffer concentration is shown in Figure S1. The samples were centrifuged, and the supernatants and the precipitates were respectively analyzed by dPAGE as schematically shown in Figure 1B.

Figure 1C shows the supernatants at pH 6. Lane 1 is the untreated DNA, while lane 2 is the heat treated sample without metal ions and it showed the highest degradation attributed to the acidity of water and high temperature. Figure 1E shows the precipitates of the pH 6 samples, where the washed precipitates were treated with EDTA and then loaded to the gel.  $\text{Mg}^{2+}$  did not form precipitate with the DNA (so no bands in Figure 1E), but it still protected the DNA. All the metal ions protected the DNA to some extent.  $\text{Cu}^{2+}$ ,  $\text{Cd}^{2+}$  and  $\text{Ce}^{3+}$  precipitated most of the DNA and protected it, although some cleavage was observed with  $\text{Cu}^{2+}$  and  $\text{Ce}^{3+}$ .  $\text{Zn}^{2+}$ ,  $\text{Co}^{2+}$ ,  $\text{Mn}^{2+}$ , and  $\text{Ni}^{2+}$  had a similar DNA content in the supernatants and in the precipitates with little degradation products observed.  $\text{Pb}^{2+}$  extensively cleaved the DNA and the cleavage products were mainly in the precipitates. The  $\text{Pb}^{2+}$  cleavage product distribution was different compared to that in the metal-free sample. Thus,  $\text{Pb}^{2+}$  cleaved the DNA in a different way.

The fluorescence of the  $\text{Fe}^{2+}$  samples nearly fully disappeared both in the supernatant and in the precipitate, which can be attributed to DNA assembly with  $\text{Fe}^{2+}$  to form Fe/DNA NPs. The formed Fe/DNA NPs did not dissolve in the presence of EDTA, indicating its ultrahigh stability. Taken together, the effect of these metal ions at pH 6.0 can be divided into four categories:

protection, cleavage, self-assembly into NPs that can be dissolved by EDTA, and that cannot be dissolved by EDTA (Figure 2A).

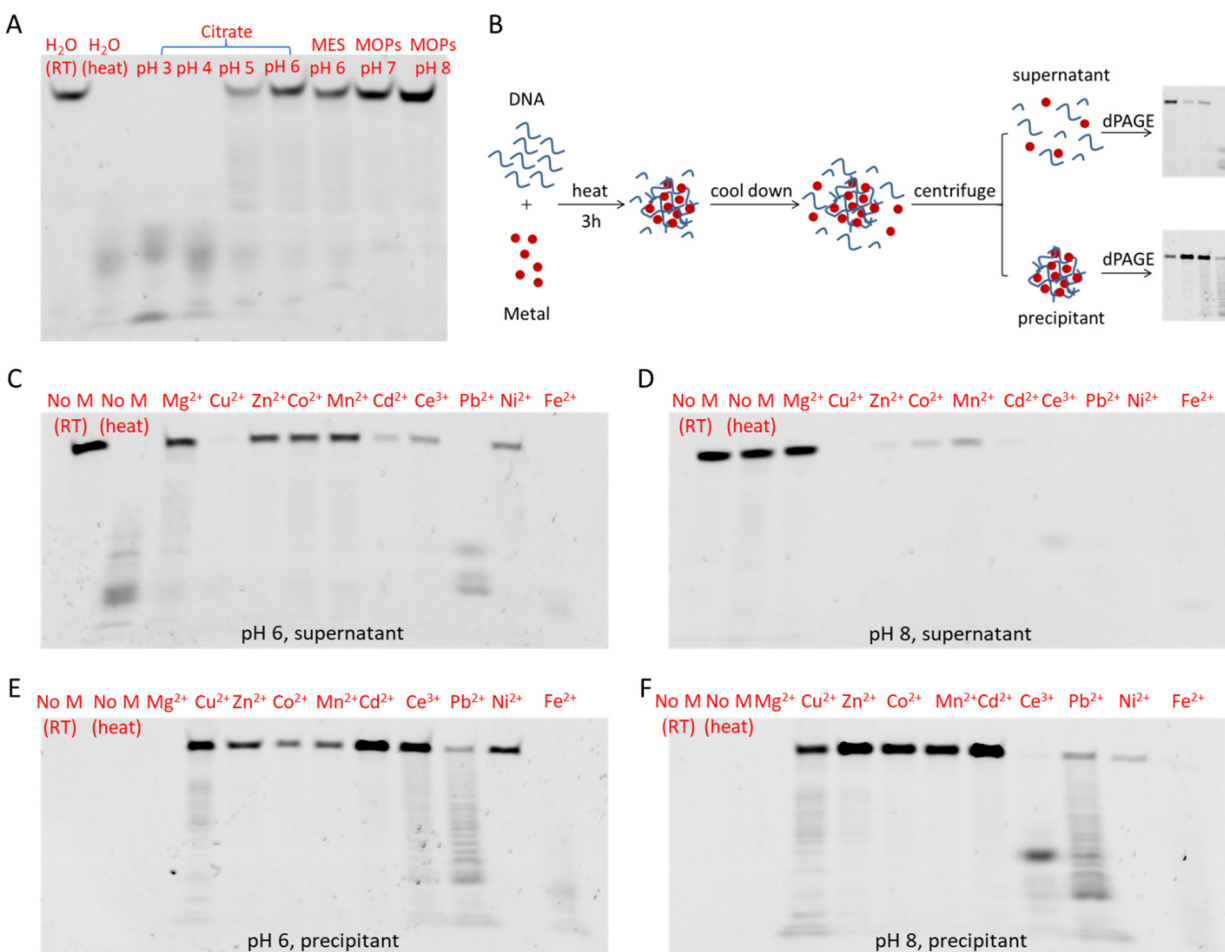


**Figure 1.** (A) FAM-24mer (1  $\mu$ M) incubated in buffers of different pH at 95°C for 3 h. The pH was adjusted using 50 mM buffer. (B) A scheme showing the experimental method. The gel micrographs of the FAM-24mer DNA mix with 4 mM different metal ions at 95 °C for 3 h in 5 mM (C, E) pH 6 MES buffer and (D, F) pH 8 MOPS buffer for the supernatants (C, D) and washed precipitates (E, F). The DNA concentration was 1  $\mu$ M FAM-24mer mixed with 3  $\mu$ M non-labeled DNA of the same sequence.

**Metal/DNA nanoparticles formed at 95°C (pH 8.0).** We then did the same experiment in a pH 8 buffer (5 mM MOPS), where the DNA in the metal-free condition was stable (Figure 1D, F). Interestingly, most of the transition metals ( $\text{Cu}^{2+}$ ,  $\text{Zn}^{2+}$ ,  $\text{Co}^{2+}$ ,  $\text{Mn}^{2+}$ ,  $\text{Cd}^{2+}$ ) nearly fully precipitated and protected the DNA, indicating that a higher pH favored DNA/metal self-

assembly.  $\text{Cu}^{2+}$  still induced a fraction of DNA degradation, and  $\text{Ce}^{3+}$  and  $\text{Pb}^{2+}$  induced full degradation of the DNA. These metals are known for their activities in cleaving DNA.<sup>14</sup> Interestingly,  $\text{Ce}^{3+}$  also fully degraded the DNA at pH 8, indicating its cleavage activity required a high pH.<sup>35</sup>  $\text{Ni}^{2+}$  and  $\text{Fe}^{2+}$  behaved similarly at pH 8, where both metals showed almost no band either in the supernatant or the precipitate. We reasoned that DNA formed highly stable NPs with them, which were not dissolved by EDTA. Thus, to prepare transition metal/DNA NPs, pH 8 can result in a higher yield. At pH 8, we can also classify the metals into four categories: no precipitation ( $\text{Mg}^{2+}$ ), precipitation and full protection, precipitation and degradation ( $\text{Ce}^{3+}$  and  $\text{Pb}^{2+}$ ), and highly stable precipitates ( $\text{Ni}^{2+}$  and  $\text{Fe}^{2+}$ ) (Figure 2A).

The TEM micrographs of a few NPs are shown in Figure 2B-E. The  $\text{Mn}^{2+}$  NPs had a rough surface, whereas the  $\text{Fe}^{2+}$  NPs were smoother. Since  $\text{Fe}^{2+}$  is quickly oxidized at basic pH, we prepared its sample in water as described in the literature.<sup>20</sup> Based on the above experiments at pH 6 and pH 8, we chose  $\text{Mg}^{2+}$ ,  $\text{Mn}^{2+}$ ,  $\text{Fe}^{2+}$  and  $\text{Pb}^{2+}$  for further studies, since they each represent a different type of metal ion.

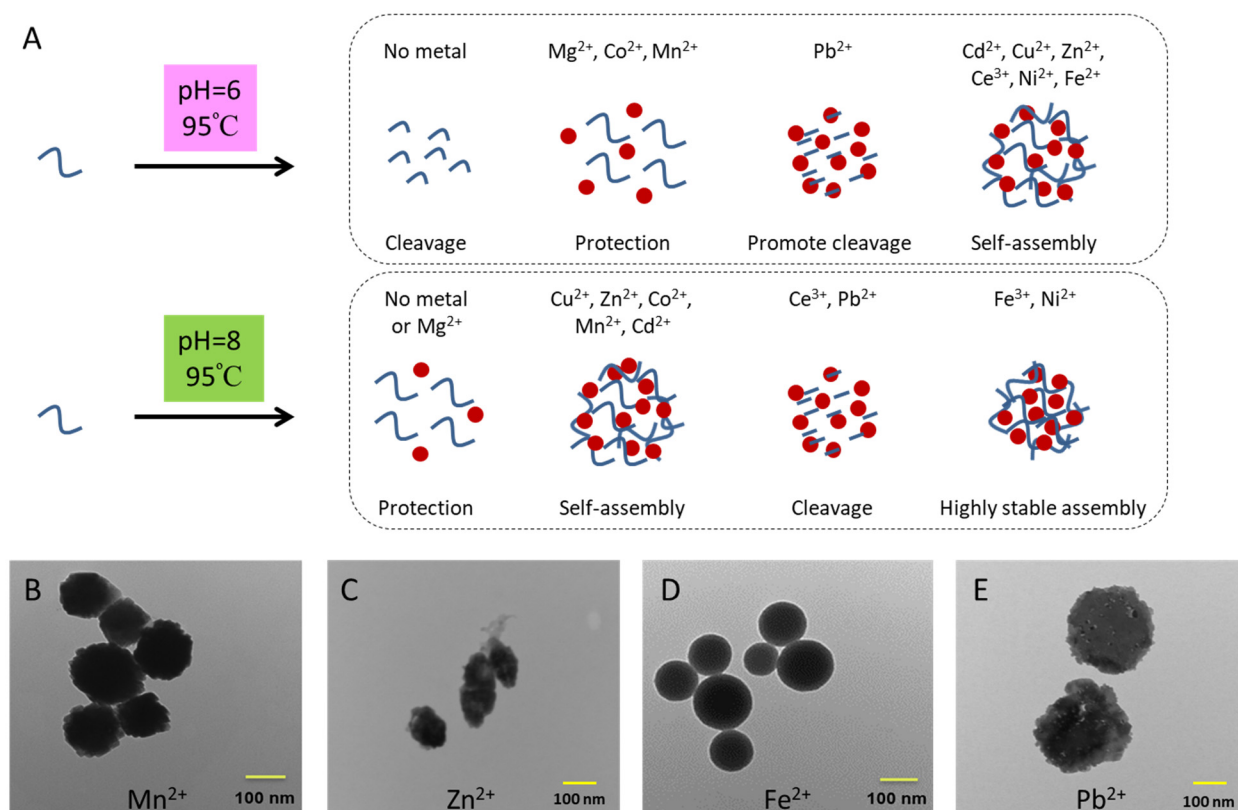


**Figure 2.** (A) Classification of the effect of metal ions by incubating them with the DNA at 95°C for 3 h at pH 6 and pH 8. TEM micrographs of nanoparticles formed by the 24-mer DNA and (B)

Mn<sup>2+</sup>, (C) Zn<sup>2+</sup>, (D) Fe<sup>2+</sup>, (E) Pb<sup>2+</sup>. The Fe<sup>2+</sup> NPs were prepared in water and the rest were in 5 mM MOPS buffer at pH 8.

**Protection of DNA by Mg<sup>2+</sup>.** Mg<sup>2+</sup> plays a critical role in nucleic acids chemistry.<sup>36-38</sup> Since Mg<sup>2+</sup> protected the DNA at high temperature, we then studied its concentration effect. After heating for 3 h at 95°C, the extent of DNA protection correlated with Mg<sup>2+</sup> concentration (Figure 3A), confirming the protection role of Mg<sup>2+</sup>. If we only heated the sample for 1 h, even 0.1 mM Mg<sup>2+</sup> achieved nearly full protection (Figure S2), indicating that the kinetics of DNA degradation was slow. We quantified the remaining fluorescence intensity as a function of Mg<sup>2+</sup> concentration, and a higher Mg<sup>2+</sup> concentration favored the protection (Figure 3B). With 3 h heating, excellent protection was achieved with 4 mM Mg<sup>2+</sup>.

We then decreased the DNA concentration by using only 0.4 μM FAM-24mer DNA (no non-labeled DNA, Figure 3C). In this case, the protection effect of Mg<sup>2+</sup> decreased significantly, and a full protection was achieved only when the Mg<sup>2+</sup> concentration was raised to 200 mM. Thus, a 10-fold drop in DNA concentration required a 50-fold increase in Mg<sup>2+</sup> for compensation. Since the protection effect was more obvious at both higher DNA concentration and high Mg<sup>2+</sup> concentration, we speculated that multiple Mg<sup>2+</sup> ions assembled multiple DNA strands to achieve the protection effect. To quantitatively understand it, we measured the protection effect at various DNA concentrations with a fixed Mg<sup>2+</sup> concentration of 4 mM, and higher DNA concentration yielded more protection (Figure 3D). So, indeed multiple DNA strands need to be assembled to exert the protection effect. Otherwise, the protection of DNA should be independent of DNA concentration. The generality of the Mg<sup>2+</sup> protection effect was also verified by testing more DNA homopolymers sequences (Figure S3).

In a paper by Walther and coworkers, long single-stranded DNA prepared by rolling circle amplification showed the lower critical solution temperature (LCST) behavior by heating the DNA in the presence of Mg<sup>2+</sup> or Ca<sup>2+</sup>.<sup>39-41</sup> Phase separation was observed at high temperature and high Mg<sup>2+</sup> concentrations. They only studied up to 80°C but their DNA was much longer. We reason that heating can promote the assembly of DNA driven by hydrophobic interactions and Mg<sup>2+</sup> can screen the charge repulsion to facilitate the assembly. Under the phase separated state, inter-strand hydrophobic interactions dominated. When DNA is packed under such a condition,

the cleavage reaction was disfavored. When cooled to room temperature, such assembled structures were disassembled and no stable coordination NPs formed between DNA and  $Mg^{2+}$  at room temperature (Figure 3E).

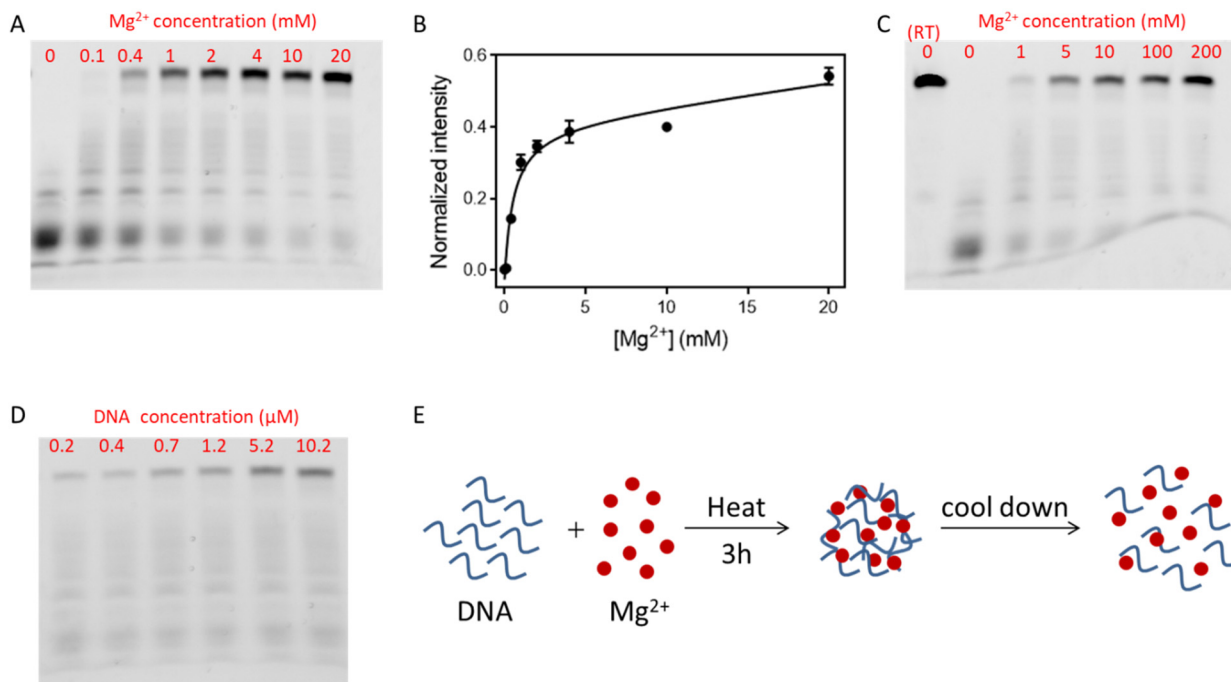


**Figure 3.** (A) A gel micrograph of FAM-24mer (1  $\mu$ M mixed with 3  $\mu$ M nonlabeled DNA) in the presence of different concentrations of  $Mg^{2+}$ . (B) Quantification of the uncleaved bands in (A). (C) Protection of 0.4  $\mu$ M FAM-24mer by different  $Mg^{2+}$  concentrations. (D) Effect of DNA concentration (0.2  $\mu$ M FAM-24mer with different concentrations of non-labeled) in the presence of 4 mM  $Mg^{2+}$ . All the samples were heated at 95  $^{\circ}$ C for 3 h. (E) A cartoon showing multiple DNA strands were assembled by  $Mg^{2+}$  to be protected at high temperature.

**Protection of DNA by assembly with  $Mn^{2+}$ .** For the next group of metal, where stable precipitates remained at room temperature (soluble with EDTA), we picked  $Mn^{2+}$  for further studies.  $Mn^{2+}$  has stronger interactions with DNA than  $Mg^{2+}$ .<sup>42</sup> Since  $Mn^{2+}$  also protected the DNA at pH 6, which was similar to  $Mg^{2+}$ , our study here focused on the formation of coordination NPs. Thus, we chose to use pH 8 to achieve a higher NP yield. After heating  $Mn^{2+}$  with the DNA, the sample turned brown with 4 mM or higher  $Mn^{2+}$  (Figure 4A, bottom panel). The effect of  $Mn^{2+}$  concentration was studied up to 20 mM (Figure 4A-C). The fraction of DNA

in the supernatants gradually decreased with increasing  $Mn^{2+}$  concentration (Figure 4C). No degradation products were observed for any of these samples.

To test the stability of the Mn/DNA NPs, we re-dispersed the precipitates and its fluorescence was quenched. After adding EDTA, KCN and KSCN, a similar amount of fluorescence increase was observed, and the highest fluorescence increase was observed in the presence of sodium triphosphate (STPP, Figure 4D). Such fluorescence increase indicated the dissolution of the Mn/DNA NPs. The fluorescence of the samples was also recorded using a digital camera with excitation at 470 nm (Figure 4D). Combining all the results, we confirmed the DNA was embedded in Mn/DNA NPs at its full length.

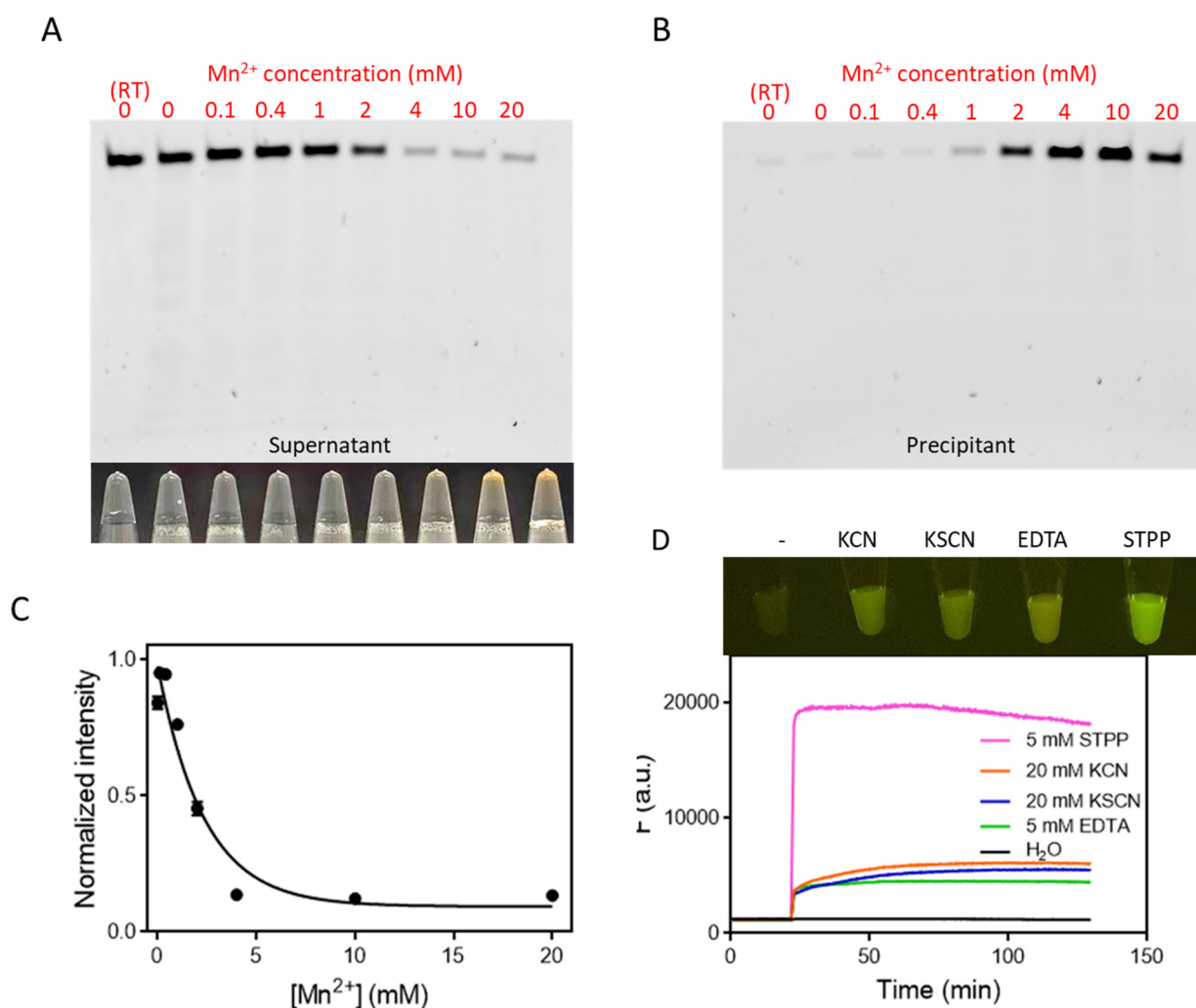


**Figure 4.** Gel micrographs showing (A) the supernatants and (B) precipitates of the FAM-24mer (1  $\mu$ M mixed with 3  $\mu$ M nonlabeled DNA of the same sequence) mix with different concentrations of  $Mn^{2+}$  at 95°C for 3 h. A photograph of the samples is also shown in (A). (C)

Quantification of the bands in (A). (D) Kinetics of fluorescence enhancement of Mn/FAM-24mer by adding various metal binding ligands. A photograph of the samples upon 470 nm excitation is also shown.

**Highly stable assembly by Fe<sup>2+</sup>.** In the above studies, the nanoparticles formed with Ni<sup>2+</sup> and Fe<sup>2+</sup> seemed to be highly stable and few DNA strands were released by EDTA and under the denaturing electrophoresis condition. Thus, we classified them as another type of metal, and examined the effect of Fe<sup>2+</sup> concentration. The overall fluorescence intensities in the gels were quite low for both the supernatants and the precipitates with more than 0.5 mM Fe<sup>2+</sup> (Figure 5A, B). With lower Fe<sup>2+</sup> concentrations, most of the DNA were cleaved. We then took the 4 mM Fe<sup>2+</sup> precipitate and added various metal chelators to observe the fluorescence enhancement (Figure 5C). Only STPP resulted in a fluorescence enhancement, whereas EDTA, KCN or KSCN failed to dissolve the Fe/DNA NPs. This was consistent with the gel electrophoresis results. The Fe/DNA NPs were extensively used for drug delivery and they can be dissolved inside cells since there are plenty of polyphosphate species inside cells.<sup>24</sup>

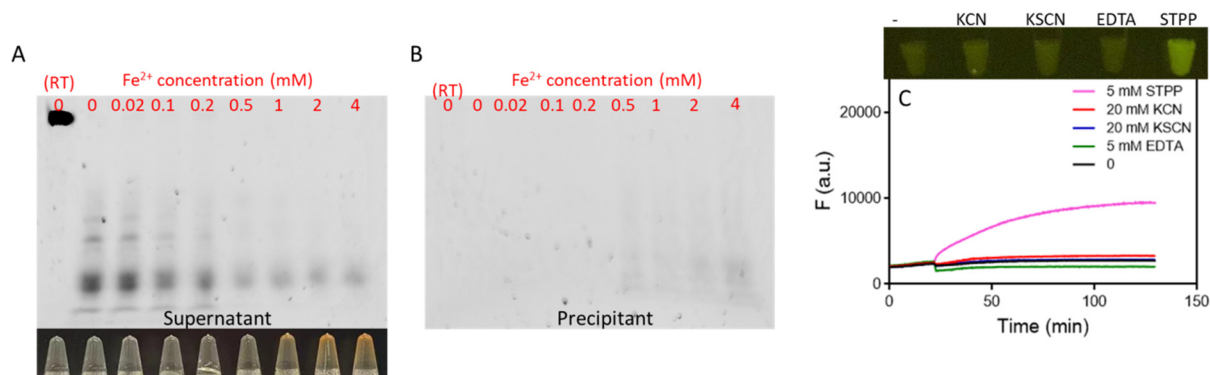


**Figure 5.** Gel micrographs showing (A) the supernatants and (B) precipitates of the FAM-24mer (1  $\mu$ M mixed with 3  $\mu$ M nonlabeled DNA of the same sequence) mixed with different concentrations of Fe<sup>2+</sup> at 95°C for 3 h. (C) Kinetics of fluorescence enhancement of Fe/FAM-24mer by adding various metal binding ligands.

**DNA cleavage by  $\text{Pb}^{2+}$ .** Finally,  $\text{Pb}^{2+}$  represents the fourth type of metal. After the heat treatment,  $\text{Pb}^{2+}$  could cleave the DNA based on our preliminary data in Figure 1. To verify this phenomenon, the effect of  $\text{Pb}^{2+}$  concentration was studied up to 4 mM (Figure 6). After heating at 95°C for 3 h, the products of degradation in the absence and presence of  $\text{Pb}^{2+}$  were quite different. The higher the  $\text{Pb}^{2+}$  concentration, the more DNA was incorporated into the precipitate. Full-length DNA was observed in all the samples as long as the  $\text{Pb}^{2+}$  concentration was higher than 0.1 mM, although the full length DNA decreased starting from 0.2 mM (Figure 6B). Since the pattern of the cleavage product was quite different for the  $\text{Pb}^{2+}$  containing and  $\text{Pb}^{2+}$  free samples,  $\text{Pb}^{2+}$ -induced degradation occurred via a different process. We reason that before  $\text{Pb}^{2+}$  could package the DNA into NPs, the degradation reaction already occurred. Degradation might further occur in the NPs.  $\text{Pb}^{2+}$  bound water has a low  $\text{p}K_a$  value and it is known to help cleave RNA.<sup>43</sup>  $\text{Pb}^{2+}$  can also bind to DNA bases, especially guanine.<sup>44</sup>

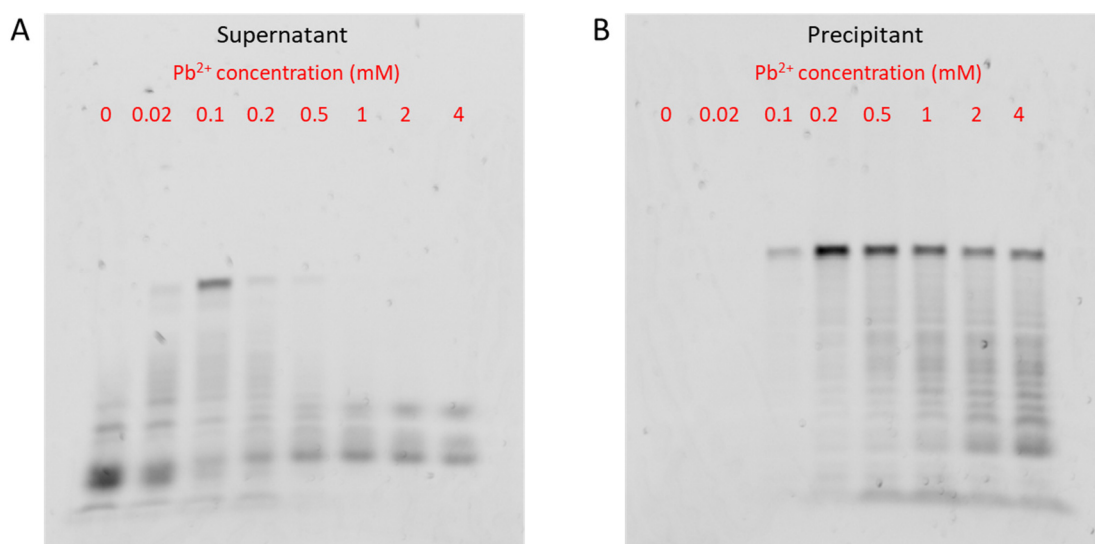


**Figure 6.** Gel micrographs of (A) the supernatants and (B) the precipitates of the FAM-24mer (1  $\mu\text{M}$  mixed with 3  $\mu\text{M}$  non-labeled DNA of the same sequence) mixed with different concentration of  $\text{Pb}^{2+}$  at 95°C for 3 h in 5 mM MES buffer, pH 6.0.

**Temperature programmed assembly.** The above characterizations were performed with gel electrophoresis. To further understand the reactions, we then followed the fluorescence intensity of FAM-24mer with 4 mM  $\text{Mg}^{2+}$  or  $\text{Mn}^{2+}$  by gradually increase the temperature in a real-time PCR thermocycler. We expected a drop in fluorescence upon forming metal/DNA coordination complexes or NPs (Figure 7A). The free DNA showed a gradual fluorescence drop due to

decreased quantum yield at higher temperature (Figure 7B, black trace).<sup>45</sup> With 4 mM  $Mg^{2+}$ , a significant drop in fluorescence was observed at round 80°C (Figure 7B, red trace), and this transition was more obvious by plotting its first derivative (Figure 7C). We attributed this transition to the formation of  $Mg^{2+}$ /DNA complexes, favoring the LCST behavior. Previous work used UV-vis spectrometry to look at the cloud point,<sup>39</sup> but a PCR thermocycler can easily access higher temperatures. With  $Mn^{2+}$ , this transition occurred at a lower temperature close to 60°C with a more significant fluorescence drop, suggesting that the  $Mn^{2+}$  complex can be formed at a lower temperature consistent with stronger  $Mn^{2+}$ /DNA interactions.

Using this method, we then varied the metal concentration. Interestingly, the transition temperatures were all around 80°C regardless of  $Mg^{2+}$  concentration (Figure 7D and Figure 7F, black dots). At a low  $Mg^{2+}$  concentration of 1 mM, the amount of DNA participated in forming the complex appeared to be lower since the peak was smaller. This can explain the less protection at lower  $Mg^{2+}$  concentrations, since the non-participated DNA strands might not be protected. We then tested the effect of  $Mn^{2+}$  concentration, and a different pattern was observed (Figure 7E). With higher  $Mn^{2+}$  concentration, the transition temperature dropped linearly (Figure 7F, red squares). It appeared that with higher concentration of  $Mn^{2+}$ , DNA can more easily be assembled, and  $Mn^{2+}$  might mediate DNA base-base interactions to achieve this.

Finally, we varied the DNA concentration. In most of the above experiments, we fixed the DNA to be 1  $\mu$ M FAM-DNA with 3  $\mu$ M non-labeled DNA to make a total of 4  $\mu$ M DNA. Here, we varied the non-labeled DNA concentration, and all the samples contained 4 mM of metal ions. Again, the transition temperatures of the  $Mg^{2+}$  samples were all around 80°C (Figure 7G, Figure 7I, black dots). For  $Mn^{2+}$ , when the DNA concentration was below 2  $\mu$ M, the transition temperature was less affected by  $Mn^{2+}$  concentration. However, the transition occurred at lower temperatures with higher  $Mn^{2+}$  concentrations (Figure 7H, Figure 7I, red triangles). This also confirmed that  $Mg^{2+}$  and  $Mn^{2+}$  are two different types of metal ions for this reaction.

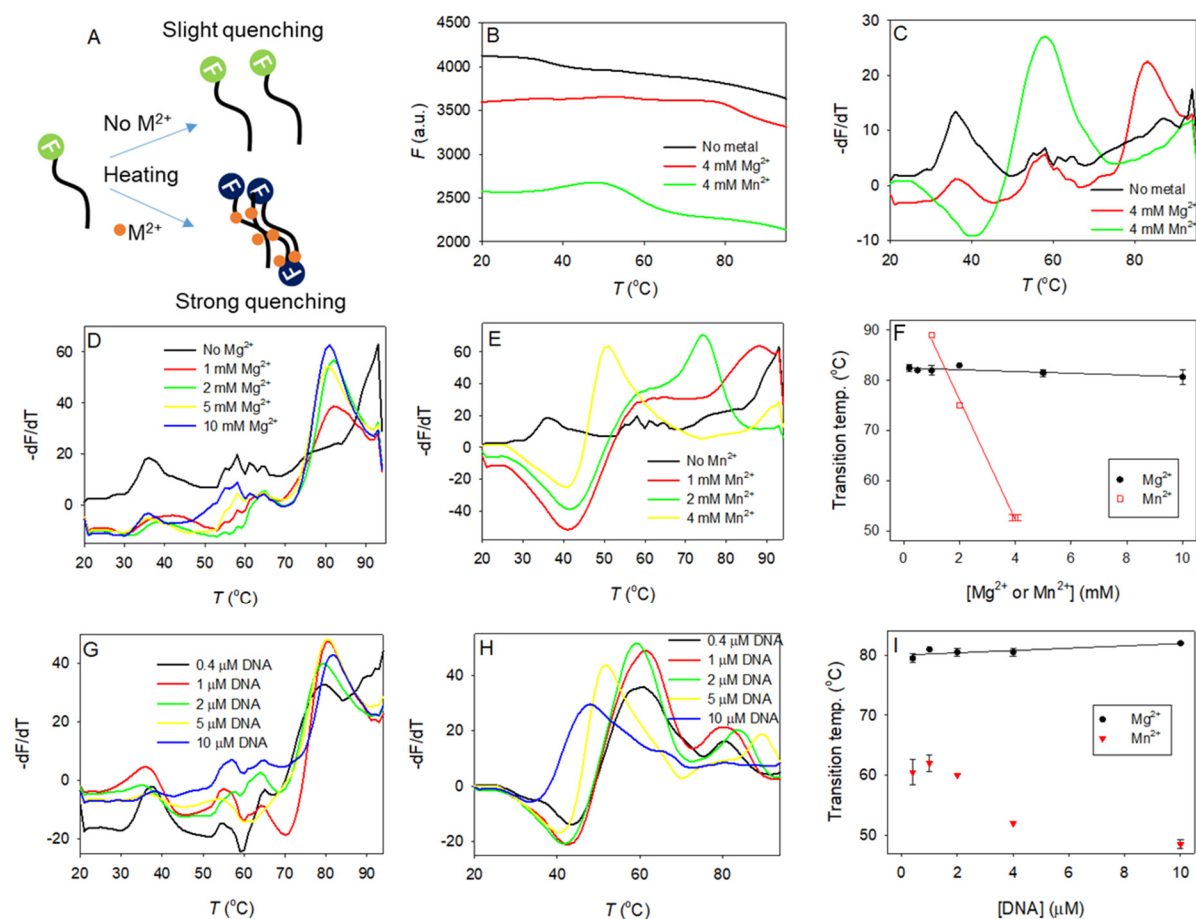


**Figure 7.** (A) A scheme showing the fluorescence change upon temperature-dependent assembly. (B) The temperature-dependent fluorescence change. (C) The first derivative of the data in (B). Effect of the concentration of (D)  $Mg^{2+}$  and (E)  $Mn^{2+}$  on the transition temperature, and (F) the change of transition temperature as a function of metal concentration. Effect of the concentration of DNA with fixed 4 mM (G)  $Mg^{2+}$  and (H)  $Mn^{2+}$  on the transition temperature, and (I) the change of transition temperature as a function of DNA concentration. All the experiments were performed with 0.4  $\mu M$  FAM-labeled DNA with 3.6  $\mu M$  non-labeled DNA of the same sequence except for the DNA concentration test. The metal concentration was 4 mM unless otherwise indicated. The buffer was 5 mM MOPS, pH 8.0.

## Discussion

In this work, we examined ten metal ions on the thermal stability of DNA oligonucleotides. Combining heating and metal ions offered DNA protection for most of the metal ions. When

heated to a very high temperature such as 95°C, the hydrophobicity of the nucleobases started to dominate.<sup>39</sup> Since DNA has a highly negatively charged phosphate backbone, metal ions are needed to screen and bridge the negative charges, contributing to the LCST behavior of DNA. When a metal ion cannot interact strongly with DNA, such as Mg<sup>2+</sup>, the assembly was only seen at high temperature, unless the formed structure was crosslinked.<sup>39</sup> With DNA base hydrophobic interactions dominating the system, the DNA adopted a different conformation leading to stabilization against high temperature. Accelerated cleavage of DNA/RNA in the presence of metal ions would typically require the position of metal ions at certain positions, such as the neutralization of the negative charges building during the transition state and providing nucleophiles.<sup>35,46</sup> However, at high temperature, the dehydration of metal ions and stronger interaction with nucleic acids may position metal ions stably at non-catalytic positions and fold DNA in conformations unfavorable for the self-cleavage reaction.

For metal ions such as Mn<sup>2+</sup> and Fe<sup>2+</sup>, they can interact with DNA stronger and the coordination interactions could remain upon cooling. Many previous work used various nucleotides and metal ions (e.g. Fe<sup>3+</sup>,<sup>47</sup> Cu<sup>2+</sup>,<sup>48</sup> Zn<sup>2+</sup>,<sup>49</sup> and lanthanides<sup>50,51</sup>) to form coordination nanoparticles,<sup>52</sup> and such metal ions are also able to coordinate with DNA.

Heating beyond the LCST of DNA in the presence of transition metal ions is a good method to prepare metal/DNA coordination materials. Mixing DNA with metal ions at room temperature would not result in such materials and heating is critical. Heating can drive DNA to assemble via hydrophobic interactions, and it can also facilitate coordination interactions (e.g. achieving inner-sphere coordination after losing water ligands of metal ions). The former brings DNA close to each other mediated by metal ions and the latter can lock the formed structures.

Both DNA<sup>53</sup> and RNA<sup>54</sup> can have catalytic activity at high temperature. The existence of hyperthermophiles also indicated the biological function of nucleic acids at high temperature. The roles of metal ions in biomolecular functions of hyperthermophiles have been noticed.<sup>55</sup> The existence of a new metal-mediated assembly of DNA at high temperature can add new insights into the discussion of the origin of life and new functions of DNA.

## Conclusions

In this work, we systematically studied the effect of metal ions on the stability of DNA oligonucleotides at a very high temperature of 95°C for up to 3 h. In contrast to the commonly

perceived cleavage of DNA, the majority of the metal ions showed a protection effect. The extent of protection is related to the strength of interaction and the chemical property of the metal ions. In general, a higher metal concentration and a higher DNA concentration are more favorable for the protection. The reason for the protection was attributed to the metal-assisted LCST behavior of DNA.  $Mg^{2+}$  has a weaker interaction and the assembled product below the LCST was unstable. Thus, at room temperature, the DNA can be released by gel electrophoresis. Some transition metal ions such as  $Mn^{2+}$  and  $Fe^{2+}$  has stronger interactions forming more stable nanoparticles.  $Pb^{2+}$ , on the other hand, promoted cleavage of the DNA. This work has broadened our fundamental understanding of nucleic acids stability at high temperature, its metal-dependent LCST behavior, and the assembly of metal-coordination nanoparticles.

### Supporting Information

The optimization of buffer concentration.

Gel micrograph for heating of 1 h.

The generality of the protection effect verified by DNA homopolymers sequences.

### Acknowledgements

Funding for this work was from the Natural Sciences and Engineering Research Council of Canada (NSERC) and the National Natural Science Foundation of China (31901776 and 32072181). C. Lu and Y. Xu received a China Scholarship Council (CSC) Scholarship to visit the University of Waterloo.

### References

1. M. R. Jones, N. C. Seeman and C. A. Mirkin, *Science*, 2015, **347**, 1260901.
2. N. C. Seeman and H. F. Sleiman, *Nat. Rev. Mater.*, 2018, **3**, 17068.
3. R. J. Lake, Z. L. Yang, J. L. Zhang and Y. Lu, *Acc. Chem. Res.*, 2019, **52**, 3275-3286.
4. D. Chang, S. Zakaria, S. Esmaeili Samani, Y. Chang, C. D. M. Filipe, L. Soleymani, J. D. Brennan, M. Liu and Y. Li, *Acc. Chem. Res.*, 2021, **54**, 3540-3549.
5. L. Wu, Y. Wang, X. Xu, Y. Liu, B. Lin, M. Zhang, J. Zhang, S. Wan, C. Yang and W. Tan, *Chem. Rev.*, 2021, **121**, 12035–12105.
6. D. Jasinski, F. Haque, D. W. Binzel and P. Guo, *ACS Nano*, 2017, **11**, 1142-1164.
7. L. Ma and J. Liu, *iScience*, 2020, **23**, 100815.

8. E. M. McConnell, I. Cozma, Q. Mou, J. D. Brennan, Y. Lu and Y. Li, *Chem. Soc. Rev.*, 2021, **50**, 8954-8994.
9. S. Mikkola, T. Lönnberg and H. Lönnberg, *Beilstein J. Org. Chem.*, 2018, **14**, 803-837.
10. Y. Li and R. R. Breaker, *J. Am. Chem. Soc.*, 1999, **121**, 5364-5372.
11. *DNA and Cell Biology*, 2013, **32**, 298-301.
12. V. I. Bruskov, L. V. Malakhova, Z. K. Masalimov and A. V. Chernikov, *Nucleic Acids Res.*, 2002, **30**, 1354-1363.
13. Y. Aiba, J. Sumaoka and M. Komiyama, *Chem. Soc. Rev.*, 2011, **40**, 5657-5668.
14. A. Sreedhara and J. A. Cowan, *J. Biol. Inorg. Chem.*, 2001, **6**, 337-347.
15. D. E. Williams and K. B. Grant, *Front. Chem.*, 2019, **7**.
16. J. Ciesiolka, in *RNA biochemistry and biotechnology*, eds. J. Barciszewski and B. F. C. Clark, Springer Netherlands, Dordrecht, 1999, pp. 111-121.
17. W. Zhou, R. Saran and J. Liu, *Chem. Rev.*, 2017, **117**, 8272-8325.
18. K. Hwang, P. Hosseinzadeh and Y. Lu, *Inorg. Chim. Acta*, 2016, **452**, 12-24.
19. X. Du, X. Zhong, W. Li, H. Li and H. Gu, *ACS Catal.*, 2018, **8**, 5996-6005.
20. M. Li, C. Wang, Z. Di, H. Li, J. Zhang, W. Xue, M. Zhao, K. Zhang, Y. Zhao and L. Li, *Angew. Chem. Int. Ed.*, 2019, **58**, 1350-1354.
21. J. Zhou, H. Han and J. Liu, *Nano Res.*, 2021, **15**, 71-84.
22. Z. Huang, B. Liu and J. Liu, *Chem. Commun.*, 2020, **56**, 4208-4211.
23. B. Liu, J. F. Zhang and L. L. Li, *Chem. Eur. J.*, 2019, **25**, 13452-13457.
24. C. Wang, Z. Di, Z. Xiang, J. Zhao and L. Li, *Nano Today*, 2021, **38**, 101140.
25. Z. Zou, L. He, X. Deng, H. Wang, Z. Huang, Q. Xue, Z. Qing, Y. Lei, R. Yang and J. Liu, *Angew. Chem. Int. Ed.*, 2021, **60**, 22970-22976.
26. Y. Bi, Z. Wang, T. Liu, D. Sun, N. Godbert, H. Li, J. Hao and X. Xin, *ACS Nano*, 2021, **15**, 15910-15919.
27. J. Li, M. Chen, S. Hou, L. Zhao, T. Zhang, A. Jiang, H. Li and J. Hao, *Carbon*, 2022, **191**, 555-562.
28. Y. Liu and Z. Tang, *Chem. Eur. J.*, 2012, **18**, 1030-1037.
29. X. Tao, Y. Peng and J. Liu, *J. Food Drug Anal.*, 2020, **28**, 575-594.
30. M. Levy and S. L. Miller, *Proc. Natl Acad. Sci. U.S.A.*, 1998, **95**, 7933-7938.
31. N. R. Pace, *Cell*, 1991, **65**, 531-533.
32. K. Matange, J. M. Tuck and A. J. Keung, *Nat. Commun.*, 2021, **12**, 1358.
33. R. An, Y. Jia, B. Wan, Y. Zhang, P. Dong, J. Li and X. Liang, *PLOS ONE*, 2015, **9**, e115950.
34. W. F. Langelier, *Journal (American Water Works Association)*, 1946, **38**, 179-185.
35. M. Komiyama, N. Takeda and H. Shigekawa, *Chem. Commun.*, 1999, 1443-1451.
36. V. K. Misra and D. E. Draper, *Proc. Natl Acad. Sci. U.S.A.*, 2001, **98**, 12456-12461.
37. R. Yamagami, J. P. Sieg and P. C. Bevilacqua, *Biochemistry*, 2021, **60**, 2374-2386.
38. R. K. O. Sigel and A. M. Pyle, *Chem. Rev.*, 2007, **107**, 97-113.
39. R. Merindol, S. Loescher, A. Samanta and A. Walther, *Nat. Nanotechnol.*, 2018, **13**, 730-738.
40. F. Xiao, Z. Chen, Z. Wei and L. Tian, *Adv. Sci.*, 2020, **7**, 2001048.
41. C. A. Mirkin and S. H. Petrosko, *Nat. Nanotechnol.*, 2018, **13**, 624-625.
42. R. K. O. Sigel and H. Sigel, *Acc. Chem. Res.*, 2010, **43**, 974-984.
43. L. S. Behlen, J. R. Sampson, A. B. DiRenzo and O. C. Uhlenbeck, *Biochemistry*, 1990, **29**, 2515-2523.

44. I. Smirnov and R. H. Shafer, *J. Mol. Biol.*, 2000, **296**, 1-5.
45. L. C. Pereira, I. C. Ferreira and M. P. F. Thomaz, *J. Photochem.*, 1978, **9**, 363-367.
46. P. Hurst, B. K. Takasaki and J. Chin, *J. Am. Chem. Soc.*, 1996, **118**, 9982-9983.
47. H. Liang, B. Liu, Q. Yuan and J. Liu, *ACS Appl. Mater. Interfaces*, 2016, **8**, 15615-15622.
48. H. Liang, F. Lin, Z. Zhang, B. Liu, S. Jiang, Q. Yuan and J. Liu, *ACS Appl. Mater. Interfaces*, 2017, **9**, 1352–1360.
49. H. Liang, Z. Zhang, Q. Yuan and J. Liu, *Chem. Commun.*, 2015, **51**, 15196-15199.
50. Q. Ma, F. Li, J. Tang, K. Meng, X. Xu and D. Yang, *Chem. Eur. J.*, 2019, **0**.
51. R. Nishiyabu, N. Hashimoto, T. Cho, K. Watanabe, T. Yasunaga, A. Endo, K. Kaneko, T. Niidome, M. Murata, C. Adachi, Y. Katayama, M. Hashizume and N. Kimizuka, *J. Am. Chem. Soc.*, 2009, **131**, 2151-2158.
52. A. Lopez and J. Liu, *ChemNanoMat*, 2017, **3**, 670–684.
53. K. E. Nelson, P. J. Bruesehoff and Y. Lu, *J. Mol. Evol.*, 2005, **61**, 216-225.
54. L. Ma, Z. Huang and J. Liu, *Chem. Commun.*, 2021, **57**, 7641-7644.
55. M. Colombo, E. Girard and B. Franzetti, *Sci. Rep.*, 2016, **6**, 20876.